Photoacoustics 24 (2021) 100302

Contents lists available at ScienceDirect

Photoacoustics

journal homepage: www.elsevier.com/locate/pacs

Research article

Activity of keloids evaluated by multimodal photoacoustic/ultrasonic imaging system

Cheng Chen [a], Sirui Liu [a], Chenyang Zhao [a], Ruojiao Wang [a], Nanze Yu [b], Xiao Long [b], Youbin Wang [b], Fang Yang [c], Jie Sun [c], Zhao Ling Lu [d], Yu Xia [a], Yuxin Jiang [a,*], Meng Yang [a,*]

[a] Department of Ultrasonography, State Key Laboratory of Complex Severe and Rare Diseases, Peking Union Medical College Hospital, Chinese Academy of Medical Sciences and Peking Union Medical College, Beijing, China
[b] Department of Plastic Surgery, Peking Union Medical College Hospital, Chinese Academy of Medical Sciences and Peking Union Medical College, Beijing, China
[c] Mindray Bio-Medical Electronics Co., Ltd., Shenzhen, China
[d] Mindray North American Innovation Center, San Jose, CA, United States

ARTICLE INFO

Keywords:
Keloids
Ultrasound
Photoacoustic imaging
Vancouver Scar Scale

ABSTRACT

Multiple objective assessments have been used to assess the activity of keloids to compare different therapeutic regimens and facilitate the best individual treatment choice for patients, but none of them are standardized. A multimodal photoacoustic/ultrasonic (PA/US) imaging system, including photoacoustic imaging, elastography, ultra-micro-angiography, and conventional US technologies (gray scale US, color Doppler US, and power Doppler US), was applied to evaluate keloids by a radiologist. Growing stages were defined by patients, and Vancouver Scar Scale (VSS) was assessed by a plastic surgeon. A comprehensive model based on multimodal ultrasound parameters (poor-echo pattern, high vascular density, decreased elasticity, and low SO_2 within the keloid) and VSS might be a potential indicator of active keloids, comparing with VSS alone. The multimodal PA/US imaging system could be a promising technique for keloids assessment.

1. Introduction

Keloids are benign dermal hyperproliferations associating with aberrant wound healing in response to cutaneous injury, and are unique to humans. These excessive scars proliferate beyond the margins of the original lesion. They commonly occur on the upper trunk, appearing as firm, thick, pigmented, pruritic, and painful nodules. The prevalent rate of keloids varies from 5% to 15 % across individuals, with a genetic predisposition to frequent occurrence in Asian and African individuals [1]. These scars can be aesthetically disfiguring and physically debilitating, leading to psychological stress and decreased life quality for patients. A number of therapeutic approaches have been applied to treat keloids. Radiotherapy after surgery is a prevalent treatment, which can effectively reduce the recurrence [2].

It is of great importance to find a method that can evaluate keloid activity, compare different therapeutic regimens, and facilitate the best individual treatment choice for patients with keloids. Various subjective and objective methods have been applied to evaluate keloids. Subjective assessments are commonly used in clinics, including the Vancouver Scar Scale (VSS), the modified Seattle scale, and standardized questionnaires; however, they are clinician and patient dependent [3,4].

This raises the need to find an objective method that not only provides precise keloid parameters but is also convenient, noninvasive, reliable, and cost-effective for clinical use. A number of tools have been applied to assess keloids, including dermoscopy [5], laser speckle contrast imaging (LSCI) [6,7], and ultrasonography (US) [8–11]. However, the accuracy of data provided by objective tools was often checked by subjective assessments in clinical practice [5–8]. Dermoscopy could visualize vascular structure, but only the upper layer tissue [5]. LSCI can provide blood perfusion, but with low penetration depth [7]. US is a widely-used imaging method in clinics and has been applied to assess keloids recently [8–11]. High-frequency US with 7.5 MHz and above is used for imaging superficial lesions with high resolution in dermatological research. Conventional US technologies include gray scale US (GSUS), color Doppler US (CDUS), and power Doppler US (PDUS). Advanced US technologies including real-time ultrasonic elastography, contrast-enhanced ultrasound (CEUS), microvessel blood flow imaging, and photoacoustic imaging (PAI) have been developing quickly.

* Corresponding authors at: Department of Ultrasonography, Peking Union Medical College Hospital, Chinese Academy of Medical Sciences and Peking Union Medical College, Address: No.1, Shuaifuyuan, Dongcheng District, Beijing, China.
E-mail addresses: jiangyuxinxh@163.com (Y. Jiang), amengameng@hotmail.com (M. Yang).

https://doi.org/10.1016/j.pacs.2021.100302
Received 23 May 2021; Received in revised form 25 August 2021; Accepted 6 September 2021

GSUS provides morphological characteristics such as echogenicity and physical parameters. Elastography detects the elasticity of tissues and has been effectively used in diagnosing breast cancer, assessing lymphedema, and evaluating skin involvement in systemic sclerosis [12–14]. CDUS and PDUS allow the presence of deep vessels and provide hemodynamic parameters. Ultra-micro-angiography (UMA) is microvessel blood flow imaging based on non-focused wave imaging technology (plane waves and divergent waves) that acquires higher time resolution than focused waves and an effective wall-filtering algorithm that distinguishes and preserves signals of low-speed tissue movement. It has the advantage of detecting low-speed blood flow and displaying microvascular morphologies.

The principle of PAI is generating thermal expansion of local tissues induced by laser irradiation, which in turn produces ultrasonic waves that can be detected by common ultrasonic probes. PAI combines the merits of optical imaging and US imaging and reflects optical characteristics of local tissue, including hemoglobin [15,16]. By detecting the hemoglobin content in local tissue, PAI can visualize microvessels and assess oxygenation by calculating the signals of deoxygenated and oxygenated hemoglobin that reach their peak absorptions at 750 nm and 830 nm wavelengths, respectively.

In this study, all these techniques were integrated into a multimodal PA/US imaging system, which has been applied in human thyroid tumors, breast tumors, and rheumatoid arthritis [17–20]. In addition, it can assess the activity of keloids and provide physical and functional parameters. Actually, there is no gold standard to assess the activity of keloids, even the pathology. Most patients come to a clinic due to the enlargement of a keloid; the activity of a keloid is defined by clinical observation, whether it became larger during the previous year [6]. This study aims to assess the activity of keloids by the multimodal PA/US imaging system, and explore a comprehensive model that is based on subjective and objective assessments.

2. Materials and methods

2.1. Patient selection

A total of 24 patients with 43 keloids were recruited from the Department of Plastic Surgery, Peking Union Medical College Hospital (PUMCH) from July 2019 to February 2021. The inclusion criteria were as follows: (1) keloids on the anterior chest, (2) keloids without prior treatment, (3) patients who can distinguish the growing stage of their keloids, and (4) patients who have been clinically evaluated by an experienced plastic surgeon. The exclusion criteria were as follows: (1) keloids with infection or bleeding, (2) spherical keloids, (3) keloids with thickness more than 10 mm above the skin, or (4) patients with concomitant systemic or regional cutaneous disease.

The study protocol was approved by the Regional Ethics Review Board of PUMCH (JS-2293), and written informed consent was obtained from each patient. All images were deidentified, and the examinations and posterior analyses followed the Helsinki principles of medical ethics.

2.2. History collection

A full history was collected before measurement, including skin type, family history, scar age, etiology, and systematic diseases of the patients. In addition, photographs (D610; Nikon, Japan) of the keloids were taken. The activity of a keloid (active, inactive) was reported by patients according to whether the keloid became larger during the previous year, based on their first impression. Group 1 (G1) and Group 2 (G2) were defined as keloids at active and inactive stages, respectively.

2.3. Clinical evaluation of keloids

VSS was evaluated by an experienced plastic surgeon before US examination. The VSS uses four variables: “pigmentation” (0 = normal, 1 = hypopigmentation, 2 = mixed pigmentation, 3 = hyperpigmentation), “vascularity” (0 = normal, 1 = pink, 2 = red, 3 = purple), “pliability” (0 = normal, 1 = supple, 2 = yielding, 3 = firm, 4 = ropes, 5 = contracture), and “height” (0 = normal/flat, 1 = < 2 mm, 2 = 2–5 mm, and 3 = >5 mm), with total score ranging from 0 to 14.

2.4. US examinations of keloids

All US examinations were performed by the same radiologist with more than 3 years of experience in dermatologic ultrasound, using commercially available ultrasonic equipment (Resona 7, Mindray Bio-Medical Electronics Co. Ltd.), equipped with an OPO tunable laser (SpitLight 600-OPO, InnoLas laser GmbH) that generated 680–980 nm laser pulses at 10 Hz. High-resolution ultrasonography was performed using a linear L9-3U probe (Mindray Bio-Medical Electronics Co. Ltd., China) with a central frequency of 5.8 MHz with 192 elements and a linear L20-5U probe (Mindray Bio-Medical Electronics Co. Ltd., China) with a central frequency of 12.9 MHz. The optical fluence on the skin for each patient was less than 20 mJ/cm^2, with fluctuations less than 5%. On PAI, there are four-in-one real-time images on the same screen (Fig. 1), including GSUS, oxygen saturation (SO_2) overlaid GSUS, and PA image at 750 nm or 830 nm overlaid GSUS. A threshold of 35 % of the maximum pixel value was applied for all PA images. PA signals below the threshold were set to be transparent in PA images and were not used for SO_2 calculation.

Patient was in a relaxed upright position, and the probe was held perpendicularly to the detected tissue, without exerting any pressure, in the transverse and longitudinal directions (Fig. 2). The multimodal PA/US imaging system allows real-time observation of the tissue (Fig. 3), and a typical active keloid and an inactive keloid were compared based on color and US images (Fig. 4). The screen could be frozen when a clear view of interesting structures was obtained.

2.4.1. GSUS assessments

Echogenicity and physical parameters were evaluated. Echogenicity of the keloid was classified into three types by comparing with fat tissue and dermis: markedly hypoechoic (poorer than fat tissue), hypoechoic (poorer than dermis), and isoechoic (close to the dermis). Parameters including total thickness, thickness above the skin, thickness penetrating into the skin (measured at the thickest point if the keloid is irregular), and length at transverse and longitudinal sections were measured.

2.4.2. Vascularity assessments

CDUS, PDUS, and UMA were combined to evaluate blood flow grading and provide hemodynamic parameters. The color gain, the pulse repetition frequency (1.0 K), and the wall filter (80 Hz) were automatically provided by the setting for superficial structures on the machine, which was configured to avoid noise. Blood flow grading was classified as: high, low, and no presence of vessels (Fig. 5). Hemodynamic parameters include peak systolic velocity (PSV) and resistance index (RI).

2.4.3. Elastography assessments

Shear wave elastography (SWE), a mode of elastography, allows quantitative elasticity assessment of the region of interest (ROI). The size of the ROI was adjusted to contain the measured keloid (K) and the adjacent skin (A). During elastography, the probe was placed on the tissue without compression, and random measurements were taken five times. For good images (credibility degree $\geq$ 95 %), the surface wave speed Cs (including Cs max, Cs mean, and Cs min) of K and A were obtained, and the ratio (K/A) was evaluated.

2.4.4. PAI assessments

PAI provides a qualitative and quantitative assessment of oxygenation state. The pixels of the PA signals at the wavelengths of 750 nm and 830 nm were measured to generate quantified values representing

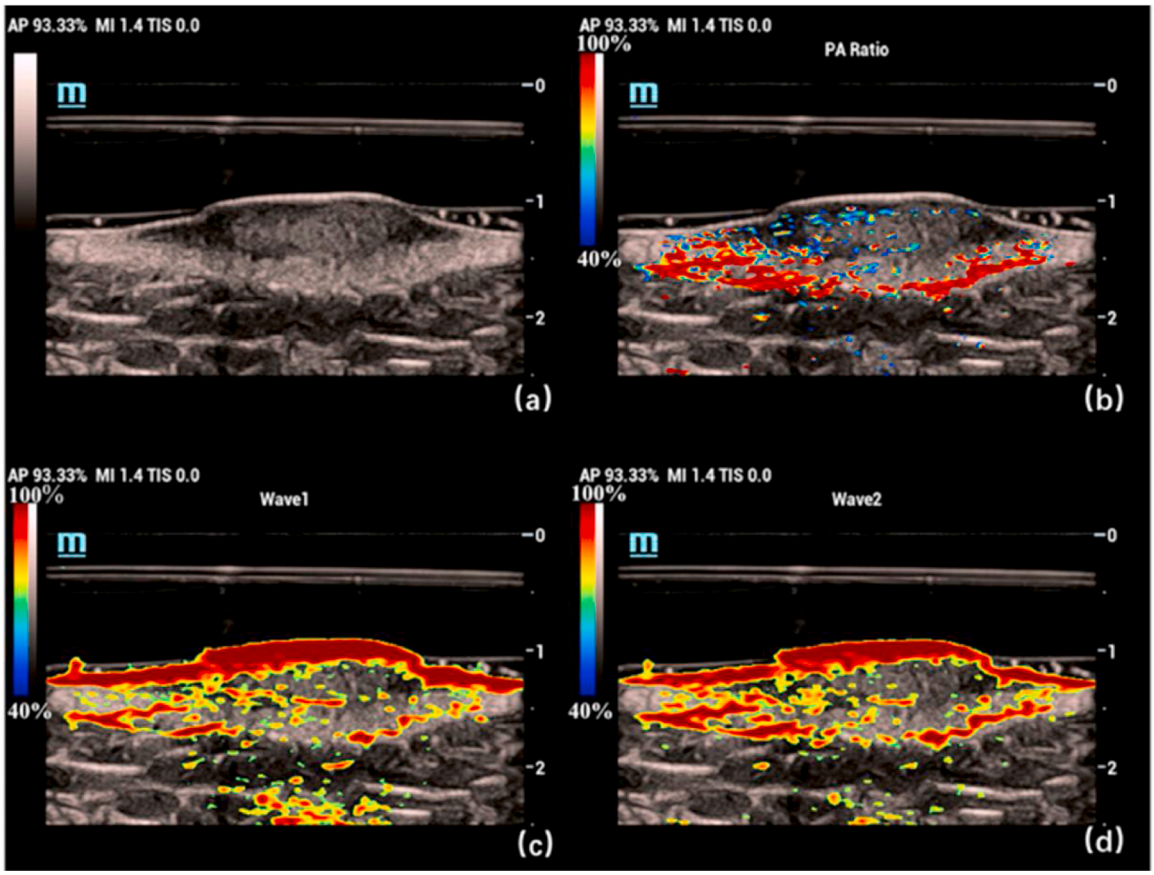

Fig. 1. Four-in-one real-time images on the same screen on PAI. (a) GSUS, (b) SO_2 overlaid GSUS, (c) PA image at 750 nm overlaid GSUS, (d) PA image at 830 nm overlaid GSUS.
GSUS: gray scale ultrasonography, PAI: photoacoustic imaging, SO_2: oxygen saturation, PA: photoacoustic.

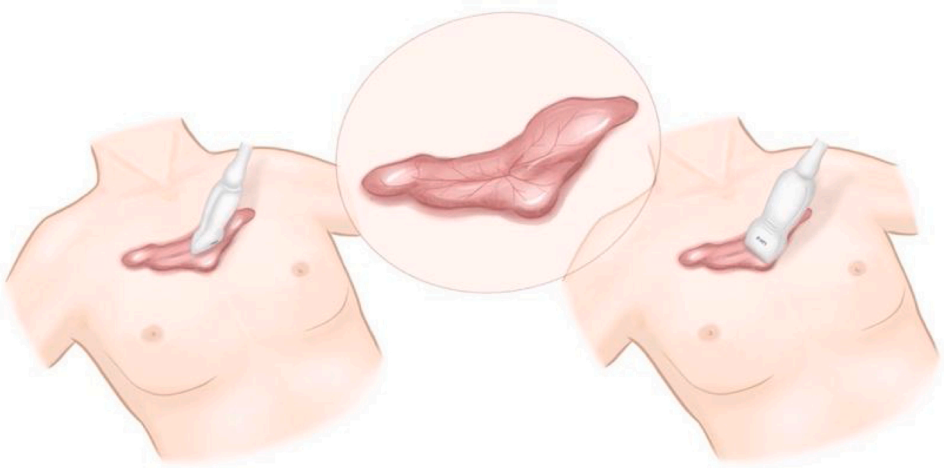

Fig. 2. The probe was placed at transverse and longitudinal directions.

oxygen saturation level of the targeted regions. Calculation of SO_2 value was conducted using built-in software in the ultrasonic platform. A gel pad was laid on the keloid before PAI to enhance imaging performance and avoid light damage. Three regions were randomly selected within each keloid and dermis. The functional maps of SO_2 are presented in a red-to-blue palette. The blue color, on one hand, indicates the lowest blood saturation level (40 %) in abnormally hypoxic tissues. The red color, on the other hand, indicates blood oxygen saturation typical of normally oxygenated tissues (100 %). In addition, it could provide a real-time SO_2 monitoring tool for measuring the SO_2 value of ROI.

2.5. Interobserver agreement

Echogenicity and blood flow grading were assessed by two radiologists with more than two years of work experience in dermatologic US, and they were blinded to the patients' information and clinical evaluation. When discrepancies were found between the two radiologists, the images would be re-confirmed and re-assessed by the two readers along

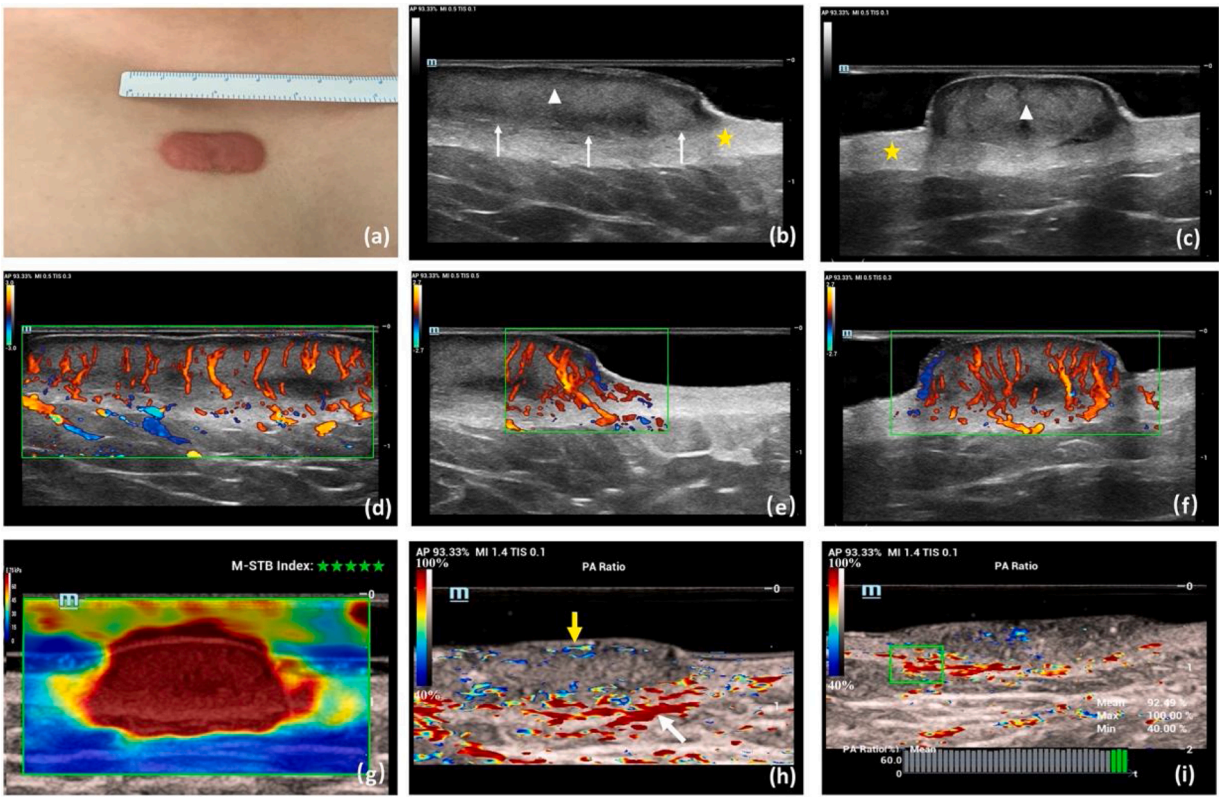

Fig. 3. Color and US images of one keloid. (a) Color image of the keloid at the anterior chest. (b) GSUS image of the keloid at transverse direction. A clear demarcation line (white arrow) was found between the keloid (white triangle) and deep/surrounding dermis tissue (yellow star). (c) GSUS image of the keloid at longitudinal direction. (d) UMA image of the keloid at transverse direction. The vessels were found emerging from the vascular network within the dermis and extending upward almost to the surface. (e) UMA image of the keloid at transverse direction. The vessels extended from the keloid margin and grew upward along the margin. (f) UMA image of the keloid at longitudinal direction. (g) Elastography indicated the keloid was harder than surrounding tissue, and it could provide quantitative elasticity. (h) PA image provided qualitative oxygenation state. The colored bars of the SO_2 images with the lowest end (blue) and the highest end (red) indicate the minimum (40 %) and the maximum (100 %) of SO_2 levels, respectively. The blue signal within the keloid revealed hypoxia (yellow arrow); the red signal below the keloid revealed hyperoxia (white arrow). (i) PA image could provide a real-time SO_2 monitoring tool for measuring the SO_2 value of ROI (green box), and the results are listed in the lower right corner of the image.
US: ultrasonography, GSUS: gray scale US, UMA: ultra-micro-angiography, ROI: region of interest, PA: photoacoustic, SO_2: oxygen saturation.

with the US operator, until consensus about the image was acquired.

2.6. Statistical evaluations

Mean and standard deviation (± SD) were used for numerical data, while frequency and percentage were used for nonnumerical data. All statistical analyses were performed by SPSS 24 (SPSS Inc. Chicago, IL, USA). In all cases, P value < 0.05 was deemed statistically significant. The normality of the data was checked by the Kolmogorov-Smirnov test. For continuous variables, independent *t*-test was used for normal distribution parameters and Wilcoxon test was used for non-normal distribution parameters. The Chi-square test or Fisher's exact test was used to compare qualitative variables between two groups. There were two types of models and no covariate: Model 1 is VSS, and model 2 is the sum of VSS and multimodal US parameters. Receiver operating characteristic (ROC) curve analyses were used to evaluate the efficacy of the two models in identifying active and inactive keloids. The area under the ROC curve (AUC) was calculated. Sensitivity and specificity were calculated. The kappa value was calculated to assess interobserver variability.

3. Results

3.1. Demographic characteristics

A total of 24 patients (12 men and 12 women with a mean age of 35.1 ± 14.4 years) with 43 keloids on the anterior chest were recruited for this study, and six of them had a positive family history. Skin types of the studied patients were III–IV. Acne was the most common cause of keloids. Of the 43 keloids, 28 (65.1 %) were active in G1 and 15 (34.9 %) were inactive in G2 (Table 1). For G1 and G2, the duration of keloid was 95.0 ± 48.5 months and 144.1 ± 49.2 months, respectively ($P = 0.003$; Table 2).

3.2. Clinical evaluation

The mean VSS values for G1 and G2 were 10.1 ± 1.8 and 5.5 ± 3.7, respectively ($P < 0.001$; Table 2).

3.3. Ultrasound measurement

3.3.1. GSUS assessments

For G1 and G2, the total thickness was 5.4 ± 1.8 mm and 5.7 ± 3.8 mm, respectively ($P = 0.743$), the thickness above the skin was 3.0 ± 1.6 mm and 2.0 ± 1.9 mm, respectively ($P = 0.042$), and the thickness penetrating into the skin was 2.5 ± 1.7 mm and 3.7 ± 3.8 mm, respectively ($P = 0.481$). Length at the transverse section was 40.4 ± 17.7 mm and 36.4 ± 33.8 mm, respectively ($P = 0.080$), and length at the longitudinal section was 19.3 ± 10.8 mm and 16.6 ± 9.5 mm, respectively ($P = 0.682$). The GSUS parameters are given in Table 2. For echogenicity, the interobserver agreement for the kappa coefficient was good, at 0.82 (95 % confidence interval [CI], 0.78–0.86). Among the 28

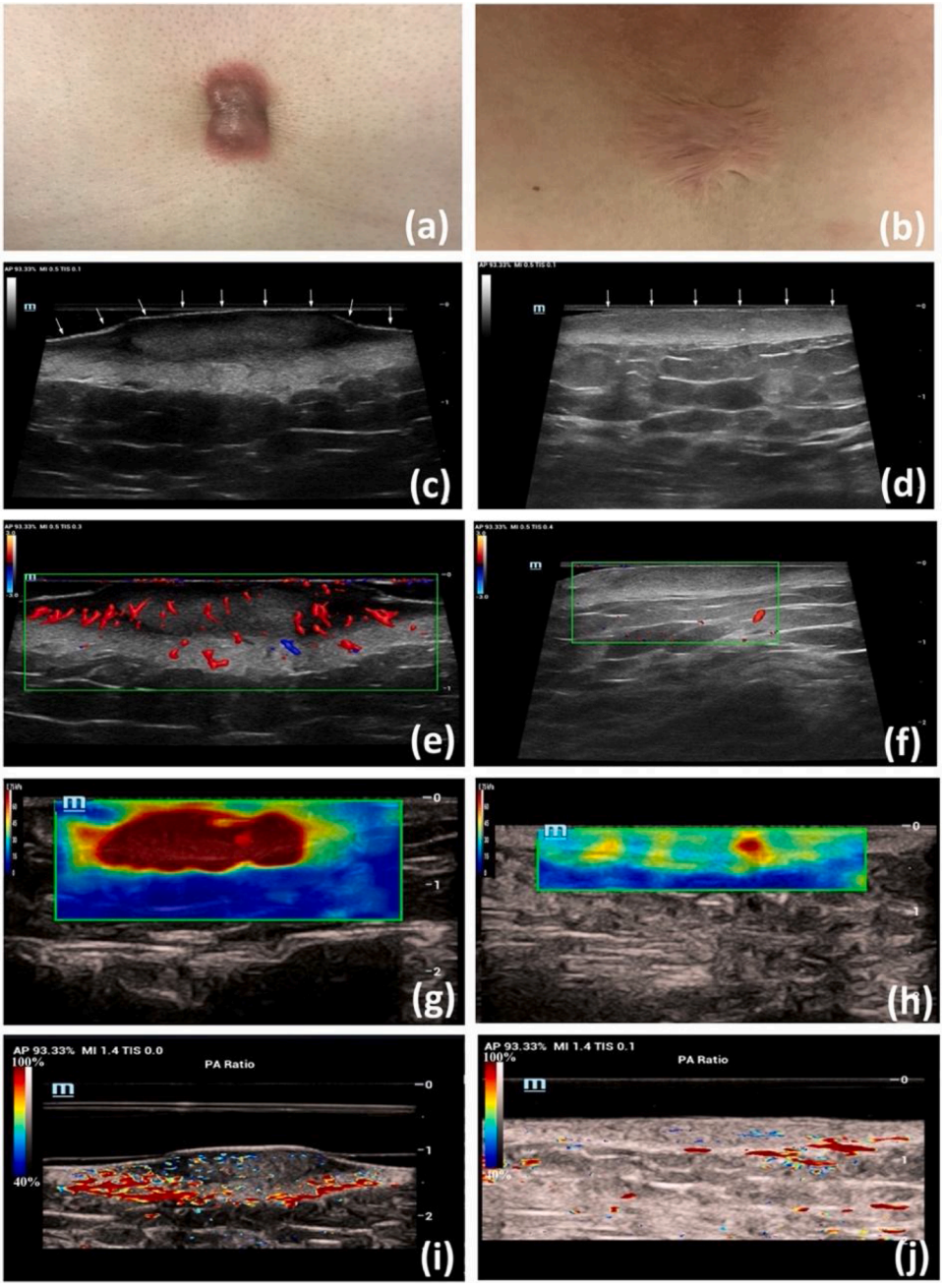

Fig. 4. A typical active keloid and an inactive keloid were compared. (a) Color image of an active keloid: It was thick and pigmented. (b) Color image of an inactive keloid: It was flat, and the color was almost normal. (c) GSUS image of an active keloid (white arrow): It was markedly hypoechoic. (d) GSUS image of an inactive keloid (white arrow): It was isoechoic. (e) UMA image of an active keloid: The blood flow grading was with high presence of vessels. (f) UMA image of an inactive keloid: The blood flow grading was with almost no presence of vessels. (g) Elastography of an active keloid: It was extremely hard. (h) Elastography of an inactive keloid. (i) PA image of an active keloid showed abundant PA signals, indicating more vasculature. (j) PA image of an inactive keloid showed sporadic PA signals, indicating less vasculature.
GSUS: gray scale ultrasonography, UMA: ultra-micro-angiography, PA: photoacoustic.

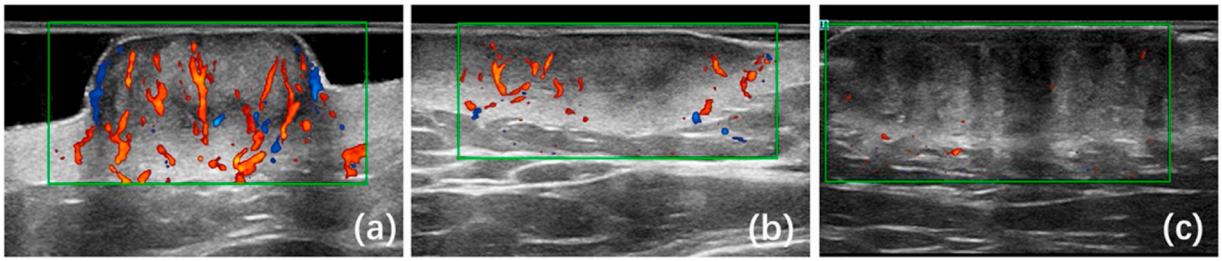

Fig. 5. Vascularity images based on UMA were used to assess vessels within the keloids. Blood flow grading was classified as: high, low, and no presence of vessels. (a) High presence of vessels: More than 10 vessels were found in one section; the vessels were emerging from the bottom to the surface. (b) Low presence of vessels: less than 10 vessels were found in one section; the vessels were short and scattered. (c) No presence of vessels.
UMA: ultra-micro-angiography.

Table 1
Demographic characteristics.

Information	
Gender	
Male	12
Female	12
Age, year	35.1 ± 14.4
Skin color (Fitzpatrick classification)	
III, patient (keloid)	23 (42)
IV, patient (keloid)	1 (1)
Stages (keloid)	
Active	28 (65.1 %)
Inactive	15 (34.9 %)

active keloids of G1, 19 (67.9 %) were markedly hypoechoic, 8 (28.6 %) were hypoechoic, and 1 (3.6 %) was isoechoic. Among the 15 inactive keloids of G2, five (33.3 %) were markedly hypoechoic, seven (46.7 %) were hypoechoic, and three (20.0 %) were isoechoic. Echogenicity between the two groups was significantly different (P = 0.046; Fig. 6a).

3.3.2. *Vascularity assessments*

For G1 and G2, the PSV was 3.0 ± 1.0 cm/s and 3.2 ± 1.2 cm/s, respectively (P = 0.664). RI was 0.4 ± 0.1 and 0.5 ± 0.1, respectively (P = 0.049). The vascularity parameters are shown in Table 2. For blood flow grading, interobserver agreement for the kappa coefficient was good, at 0.81 (95 % CI, 0.75–0.87). Among the 28 active keloids of G1, 18 (64.3 %) were with high presence of vessels, 9 (32.1 %) were with

Table 2
Clinical and Uutrasound characteristics of keloids at different stages.

	G1: Active stage (n = 28)	G2: Inactive stage (n = 15)	*P*
Duration, month	95.0 ± 48.5	144.1 ± 49.2	*0.003***
Clinical evaluation			
VSS	10.1 ± 1.8	5.5 ± 3.7	*<0.001***
Pigmentation	2.6 ± 0.6	1.1 ± 1.1	*<0.001***
Vascularization	2.0 ± 0.7	1.1 ± 1.1	*0.006**
Pliability	2.7 ± 0.7	1.7 ± 1.1	*0.005**
Height	2.9 ± 0.9	1.7 ± 1.3	*0.003***
GSUS assessments			
Total thickness (mm)	5.4 ± 1.8	5.7 ± 3.8	*0.743*
Thickness above the skin (mm)	3.0 ± 1.6	2.0 ± 1.9	*0.042**
Thickness penetrating into the skin (mm)	2.5 ± 1.7	3.7 ± 3.8	*0.481*
Length at transverse section (mm)	40.4 ± 17.7	36.4 ± 33.8	*0.080*
Length at longitudinal section (mm)	19.3 ± 10.8	16.6 ± 9.5	*0.682*
Vascularity assessments			
PSV (cm/s)	3.0 ± 1.0	3.2 ± 1.2	*0.664*
RI	0.4 ± 0.1	0.5 ± 0.1	*0.049**
Elasticity assessments			
K Cs max (m/s)	8.2 ± 1.6	6.6 ± 1.7	*0.008**
K Cs mean (m/s)	6.2 ± 1.8	5.5 ± 1.7	*0.306*
K Cs min (m/s)	4.2 ± 2.3	4.2 ± 1.7	*0.709*
K/A Cs max	2.4 ± 0.6	1.7 ± 0.6	*0.004***
K/A Cs mean	1.9 ± 0.7	1.5 ± 0.5	*0.041**
K/A Cs min	1.5 ± 0.8	1.3 ± 0.5	*0.609*
PAI assessments			
SO_2 within the keloid	78.1 %±4.7 %	82.8 %±2.3 %	*0.001***
SO_2 below the keloid	90.7 %±3.7 %	92.2 %±1.8 %	*0.102*

VSS: Vancouver Scar Scale, GSUS: gray scale ultrasonography, PSV: systolic peak velocity, RI: resistance index, Cs: surface wave speed, K: keloid, K/A: ratio of keloid to adjacent skin, SO_2: oxygen saturation.
* $P < 0.05$.
** $P < 0.005$.

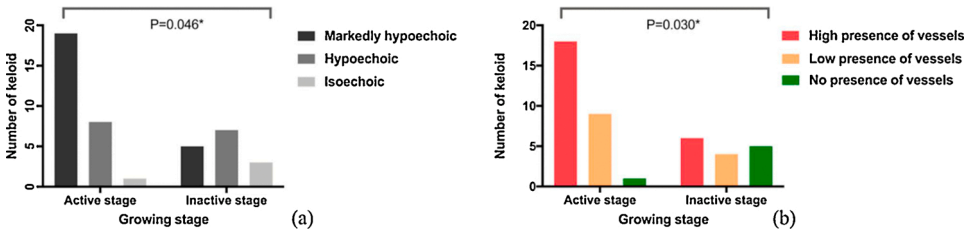

Fig. 6. Number of keloids at different stages. (a) Echogenicity of keloids at different stages, (b) Blood flow grading of keloids at different stages.

Table 3
Scores of VSS and multimodal ultrasound parameters.

	0	1	2	3	4	5
Vancouver Scar Scale						
Pigmentation	normal	hypopigmentation	mixed pigmentation	hyperpigmentation		
Vascularity	normal	pink	red	purple		
Pliability	normal	supple	yielding	firm	ropes	contracture
Height	normal	<2 mm	2–5 mm	>5 mm		
Multimodal ultrasound parameters						
Echogenicity		isoechoic	hypoechoic	markedly hypoechoic		
Blood flow grading		no presence of vessels	low presence of vessels	high presence of vessels		
K Cs max		<7.070	≥7.070			
SO_2 within the keloid		>81.04 %	≤81.04 %			

Cs: surface wave speed, K: keloid, SO_2: oxygen saturation.

low presence of vessels, and 1 (3.6 %) was with no presence of vessels. Among the 15 inactive keloids of G2, six (40.0 %) were with high presence of vessels, four (26.7 %) were with low presence of vessels, and five (33.3 %) were with no presence of vessels. Blood flow grading between the two groups was significantly different (P = 0.030; Fig. 6b).

3.3.3. Elasticity assessments

For G1 and G2, K Cs max was 8.2 ± 1.6 m/s and 6.6 ± 1.7 m/s, respectively (P = 0.008), K Cs mean was 6.2 ± 1.8 m/s and 5.5 ± 1.7 m/s, respectively (P = 0.306), K Cs min was 4.2 ± 2.3 m/s and 4.2 ± 1.7 m/s, respectively (P = 0.709). K/A Cs max was 2.4 ± 0.6 and 1.7 ± 0.6, respectively (P = 0.004), K/A Cs mean was 1.9 ± 0.7 and 1.5 ± 0.5, respectively (P = 0.041), and K/A Cs min was 1.5 ± 0.8 and 1.3 ± 0.5, respectively (P = 0.609). The elasticity parameters are given in Table 2.

3.3.4. PAI assessments

For G1 and G2, SO_2 within the keloid was 78.1 %±4.7 % and 82.8 %±2.3 %, respectively (P = 0.001), and SO_2 below the keloid was 90.7 %±3.7 % and 92.2 %±1.8 %, respectively (P = 0.102). The PAI parameters are given in Table 2.

3.4. ROC analysis

For model 1, the sensitivity and specificity were 100.0 % and 60.0 %, respectively, and the AUC was 0.907 (95 % CI, 0.798–0.984). The positive predictive value (PPV), negative predictive value (NPV), and diagnostic accuracy (ACC) were 82.4 %, 100.0 %, and 86.1 %, respectively.

For multimodal ultrasound parameters, the score of echogenicity ranged from 1 to 3 (1 = isoechoic, 2 = hypoechoic, 3 = markedly hypoechoic). The score of blood flow grading ranged from 1 to 3 (1 = no presence of vessels, 2 = low presence of vessels, 3 = high presence of vessels). The ROC curve demonstrated that a value of K Cs max of 7.070 was the best cutoff to differentiate between active and inactive keloids [AUC = 0.766 (95 %CI, 0.592–0.940); sensitivity = 71.4 %; specificity = 86.4 %]. The score of K Cs max ranged from 1 to 2 (1 = value < 7.070, 2 = value≥7.070). The ROC curve demonstrated that a value of 81.04 % for SO_2 within the keloid was the best cutoff [AUC = 0.810 (95 % CI, 0.669–0.951); sensitivity = 78.6 %; specificity = 80.0 %]. The score of SO_2 within the keloid ranged from 1 to 2 (1 = value > 81.04 %, 2 = value≤81.04 %). Multimodal ultrasound parameters include the score of echogenicity, blood flow grading, K Cs max, and SO_2 within the keloid (Table 3).

For model 2, the sensitivity and specificity were 100.0 % and 70.0 %, respectively, and the AUC was 0.950 (95 % CI, 0.889–1.000). PPV, NPV, and ACC were 100.0 %, 68.4 %, and 81.8 %, respectively. The ROC curves of VSS, and multimodal ultrasound parameters and VSS are shown in Fig. 7a and b, respectively.

4. Discussion

There is currently no gold standard to accurately evaluate keloid activity, including pathology. Moreover, invasive operation is contraindicated since it will increase the size or activity of keloids. Therefore, it is important to find a noninvasive method that can provide reliable evaluation of keloid activity and assess therapeutic effects. US, one of

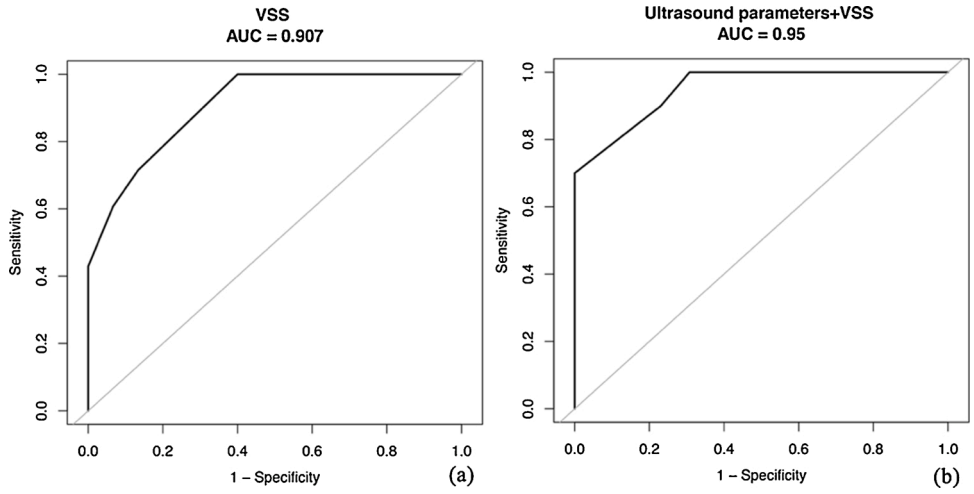

Fig. 7. ROC curves of two models in the evaluation of keloid activity. (a) Model 1 is VSS. (b) Model 2 is the sum of multimodal ultrasound parameters and VSS. ROC: receiver operating characteristic.

the first-line clinical examination techniques, allows noninvasive evaluation of skin and subcutaneous tissues with high resolution; however, only one or several US technologies were used to evaluate keloids in previous studies. Recently, new US technologies such as UMA, elastography, and PAI have been developing quickly, which can provide vital information for keloids. Favorably, all these technologies can be integrated into multimodal PA/US imaging system. To our knowledge, this is the first study to assess the activity of keloids *via* a multimodal PA/US imaging system, providing morphological and functional properties. Moreover, L9-3U and L20-5U probes are able to offer not only sufficient penetration depth but also high resolution in dermatological research.

In clinics, total thickness and thickness penetrating into the skin are hard to evaluate, and thickness above the skin may be affected by adjacent keloids or surrounding contractures of skin. GSUS assessment provides accurate thickness and length at all sections of keloids for monitoring its variation [11]. Moreover, echogenicity indicates the ability of tissues to reflect sound waves, and it was classified into three types in this study. Characterized by excessive collagen deposition, keloids were previously expected to be hyperechoic lesions. This study revealed that active keloids have a poorer echo than inactive keloids. Active keloids were mainly markedly hypoechoic, while inactive keloids were mainly hypoechoic. Echogenicity of keloids may depend on the prominent hypoechoic extracellular matrix (ECM) components or the prominent hyperechoic dense collagen bundles within keloids. The physiologic wound healing cascade includes inflammation, proliferation, and remodeling. Active keloids correspond to the inflammation and proliferation phases, with increased water-binding properties, abundant ECM components, and high vascularity density [8,21]. Inactive keloids correspond to the remodeling phase, with collagen deposition occurring in an organized fashion [8,21]. To some degree, echogenicity is able to reflect the growth status of keloids.

Literatures reveal that angiogenesis may play a role in the pathogenesis of keloids, and vascularity may relate to the activity of keloids [6,9,22]. Oxygen consumption within keloids is high (due to inflammation, increased collagen synthesis, enlarged endothelial cells, and fibroblast proliferation), while oxygen supply is relatively low (due to narrowing or occlusive micro-vessels) [23–26]. Keloids consume more oxygen than microvessels can supply, resulting in relatively hypoxic conditions. Under such low oxygen concentrations, hypoxia-inducible factor 1α (HIF-1α) increases and upregulates vascular endothelial growth factor expression, which promotes angiogenesis and enhances hypoxia tolerance [27]. In clinics, the color of keloids is commonly used as an indicator of vascularity [28,29]; however, it is sometimes difficult to assess accurately due to post-inflammatory pigmentation or different skin types. Conventional CDUS and PDUS have been applied to evaluate the activity of keloids [8,9], although they are not sensitive enough to observe low blood flow and microvascularity [30]. Owing to an excess of endothelial cells, keloids usually present with low-velocity vessels due to narrowing or occlusive microvessels [31,32]. This is the first study that utilizes UMA to assess angiogenesis of keloids, with increased sensitivity for low-velocity blood flow. This study showed that active keloids have more blood flow and lower RI than inactive keloids, consistent with a previous study [9]. Moreover, a combination of CDUS, PDUS, and UMA is ideal for assessing keloid vascularity.

Elasticity assessment revealed that keloids are harder than normal skin, and active keloids are harder than inactive keloids. Keloids are composed of excess collagen in a discrete nodule, leading to increased hardness and decreased elasticity. Improved elasticity is considered as an objective parameter denoting successful treatment, in accordance with a previous study [33]. Elasticity detected by US is a reliable and effective objective reflection of keloid stiffness. However, keloids are often described as having an actively growing peripheral margin with a regressing center. This heterogeneity may result in an uneven keloid surface. Although the probe was maintained perpendicular to the tissue as lightly as possible during examination, the contact between the probe and keloid may be affected by the uneven surface. In this study, each keloid was measured five times, and the probe had a small surface area to minimize the error. The ratio of keloid to adjacent skin was calculated to reduce differences between individuals.

As mentioned above, angiogenesis is promoted and hypoxia tolerance is enhanced within keloids. It is essential to evaluate the actual oxygenation state as it may reflect the activity of keloids. Sloan [34] inserted a stainless steel gas probe into scar tissue and indicated that oxygen pressure in a hypertrophic scar was lower than that in normal skin; however, it is time-consuming and invasive. Shigeru [35] used an original system equipped with a Clark oxygen electrode and demonstrated high oxygen consumption of *ex vivo* keloid tissue, but it is not suitable for use in humans. Actually, the oxygenation state of *in vivo* keloids has never before been non-invasively presented. In this study, the utility of PAI demonstrated that *in vivo* keloids were hypoxic. Moreover, active keloids had lower SO_2 than inactive keloids, which is consistent with previous studies that reported on the high oxygen consumption rate of keloids and comparatively low consumption rate of mature scars [35]. Recently, some researches have revealed that hyperbaric oxygen therapy (HBOT) can greatly improve keloid condition and provide effective treatment, as it may inhibit HIF-1α expression [36,37]. As a result, timely HBOT intervention could reduce keloid recurrence rate. PAI might be helpful in monitoring SO_2 variation when taking HBOT, which could be further investigated.

This is the first study that established a comprehensive model based on imaging system and clinical evaluation. VSS is the most widely used scoring system to evaluate keloids and assess their degrees of improvement based on clinical parameters; however, they are totally clinician dependent. Comparatively, multimodal PA/US imaging system can provide objective qualitative and quantitative data, including echogenicity, blood flow grading, elasticity, and oxygenation state. The imaging system can effectively improve subjective assessment, and subjective assessments cannot be replaced. As shown in this study, the model based on both multimodal PA/US imaging system and VSS is effective in predicting the activity of keloids.

To reduce bias, all keloids assessed in this study were on the anterior chest and without prior treatment, as the majority of keloids are prone to grow on the anterior chest, and the growth of keloids on the anterior chest could be easily observed by patients. Based on the extracted data, further research will be done to evaluate heterogeneous keloids all over the body. However, some limitations exist in the current study, such as a relatively small number of enrolled patients and a lack of follow-up. Moreover, the classification is based on clinical observation. Larger, longer, and in-depth studies are still necessary to investigate the multimodal PA/US imaging system and verify the model we have established, and more research is needed to evaluate treatment efficiency and to compare different treatment regimens.

In conclusion, multimodal PA/US imaging system with high resolution might be a promising and reliable device to assess the activity of keloids in clinics. The model based on multimodal ultrasound parameters (poor-echo pattern, high vascular density, decreased elasticity, and low SO_2 within the keloid) and VSS might be a potential indicator of active keloids.

Author contributions

Cheng Chen, Meng Yang, and Yuxin Jiang conceived the idea of the study. Nanze Yu, Xiao Long, and Youbin Wang are plastic surgeons, who recruited the patients. Cheng Chen performed multimodal PA/US imaging system. Fang Yang, Jie Sun, and Zhao Ling Lu are engineers, who provided technical support. Data collection was completed and analyzed by Cheng Chen, Sirui Liu, Chenyang Zhao, Ruojiao Wang, and Yu Xia. Cheng Chen wrote the first draft of the manuscript. Meng Yang received the fundings. The manuscript was critically reviewed by all authors.

Funding

This work was funded by the Beijing Natural Science Foundation (JQ18023); the National Natural Science Foundation of China (61971447); Beijing Nova Program Interdisciplinary Cooperation Project (xxjc2018023); CAMS Innovation Fund for Medical Sciences (CIFMS) (2020-I2M-C&T-B-035); National Key Research and Development Program from the Ministry of Science and Technology of the People's Republic of China (2017YFE0104200); and International Science and Technology Cooperation Programme (2015DFA30440).

Declaration of Competing Interest

The authors declare that there are no conflicts of interest.

References

[1] B. Berman, V.L. Young, J. McAndrews, Objective assessment of the precision, accuracy, and reliability of a measurement method for keloid scar volume (PARKS study), Dermatol. Surg. 41 (11) (2015) 1274–1282.
[2] M. Emad, S. Omidvari, L. Dastgheib, A. Mortazavi, H. Ghaem, Surgical excision and immediate postoperative radiotherapy versus cryotherapy and intralesional steroids in the management of keloids: a prospective clinical trial, Med. Princ. Pract. 19 (5) (2010) 402–405.
[3] J.P. Andrews, J. Marttala, E. Macarak, J. Rosenbloom, J. Uitto, Keloids: the paradigm of skin fibrosis - pathomechanisms and treatment, Matrix Biol. 51 (2016) 37–46.
[4] M.H. Viera, A.C. Vivas, B. Berman, Update on keloid management: clinical and basic science advances, Adv. Wound Care (New Rochelle) 1 (5) (2012) 200–206.
[5] M.G. Yoo, I.H. Kim, Keloids and hypertrophic scars: characteristic vascular structures visualized by using dermoscopy, Ann. Dermatol. 26 (5) (2014) 603–609.
[6] C. Chen, M. Zhang, N. Yu, W. Zhang, X. Long, Y. Wang, X. Wang, Heterogeneous features of keloids assessed by laser speckle contrast imaging: a cross-sectional study, Lasers Surg. Med. 53 (6) (2021) 865–871.
[7] Q. Liu, X. Wang, Y. Jia, X. Long, N. Yu, Y. Wang, B. Chen, Increased blood flow in keloids and adjacent skin revealed by laser speckle contrast imaging, Lasers Surg. Med. 48 (4) (2016) 360–364.
[8] A.M. Elrefaie, R.M. Salem, M.H. Faheem, High-resolution ultrasound for keloids and hypertrophic scar assessment, Lasers Med. Sci. 35 (2) (2020) 379–385.
[9] N. Lobos, X. Wortsman, F. Valenzuela, F. Alonso, Color doppler ultrasound assessment of activity in keloids, Dermatol. Surg. 43 (6) (2017) 817–825.
[10] H. Schwaiger, M. Reinholz, J. Poetschke, T. Ruzicka, G. Gauglitz, Evaluating the therapeutic success of keloids treated with cryotherapy and intralesional corticosteroids using noninvasive objective measures, Dermatol. Surg. 44 (5) (2018) 635–644.
[11] H.D. Gamil, F.M. Khattab, M.M. El Fawal, S.E. Eldeeb, Comparison of intralesional triamcinolone acetonide, botulinum toxin type A, and their combination for the treatment of keloid lesions, J. Dermatolog. Treat. (2019) 1–10.
[12] J.R. Grajo, R.G. Barr, Strain elastography for prediction of breast cancer tumor grades, J. Ultrasound Med. 33 (1) (2014) 129–134.
[13] A. Iagnocco, O. Kaloudi, C. Perella, F. Bandinelli, V. Riccieri, M. Vasile, F. Porta, G. Valesini, M. Matucci-Cerinic, Ultrasound elastography assessment of skin involvement in systemic sclerosis: lights and shadows, J. Rheumatol. 37 (8) (2010) 1688–1691.
[14] A.J. Forte, M.T. Huayllani, D. Boczar, G. Cinotto, S.A. McLaughlin, Ultrasound elastography use in lower extremity lymphedema: a systematic review of the literature, Cureus 11 (9) (2019) e5578.
[15] L.V. Wang, S. Hu, Photoacoustic tomography: in vivo imaging from organelles to organs, Science (New York, N.Y.) 335 (6075) (2012) 1458–1462.
[16] C. Li, L.V. Wang, Photoacoustic tomography and sensing in biomedicine, Phys. Med. Biol. 54 (19) (2009) R59–97.
[17] R. Zhang, L.Y. Zhao, C.Y. Zhao, M. Wang, S.R. Liu, J.C. Li, R.N. Zhao, R.J. Wang, F. Yang, L. Zhu, X.J. He, C.H. Li, Y.X. Jiang, M. Yang, Exploring the diagnostic value of photoacoustic imaging for breast cancer: the identification of regional photoacoustic signal differences of breast tumors, Biomed. Opt. Express 12 (3) (2021) 1407–1421.
[18] C. Zhao, Q. Wang, X. Tao, M. Wang, C. Yu, S. Liu, M. Li, X. Tian, Z. Qi, J. Li, F. Yang, L. Zhu, X. He, X. Zeng, Y. Jiang, M. Yang, Multimodal photoacoustic/ultrasonic imaging system: a promising imaging method for the evaluation of disease activity in rheumatoid arthritis, Eur. Radiol. 31 (5) (2021) 3542–3552.
[19] M. Yang, L. Zhao, X. He, N. Su, C. Zhao, H. Tang, T. Hong, W. Li, F. Yang, L. Lin, B. Zhang, R. Zhang, Y. Jiang, C. Li, Photoacoustic/ultrasound dual imaging of human thyroid cancers: an initial clinical study, Biomed. Opt. Express 8 (7) (2017) 3449–3457.
[20] M. Yang, L. Zhao, F. Yang, M. Wang, N. Su, C. Zhao, Y. Gui, Y. Wei, R. Zhang, J. Li, T. Han, X. He, L. Zhu, H. Wu, C. Li, Y. Jiang, Quantitative analysis of breast tumours aided by three-dimensional photoacoustic/ultrasound functional imaging, Sci. Rep. 10 (1) (2020) 8047.
[21] M.N. Bessonart, N. Macedo, C. Carmona, High resolution B-scan ultrasound of hypertrophic scars, Skin Res. Technol. 11 (3) (2005) 185–188.
[22] Y. Kang, M.R. Roh, S. Rajadurai, A. Rajadurai, R. Kumar, C.N. Njauw, Z. Zheng, H. Tsao, Hypoxia and HIF-1α regulate collagen production in keloids, J. Invest. Dermatol. 140 (11) (2020) 2157–2165.
[23] Z. Barjaktarovic, D. Schmaltz, A. Shyla, O. Azimzadeh, S. Schulz, J. Haagen, W. Dorr, H. Sarioglu, A. Schafer, M.J. Atkinson, H. Zischka, S. Tapio, Radiation-induced signaling results in mitochondrial impairment in mouse heart at 4 weeks after exposure to X-rays, PLoS One 6 (12) (2011), e27811.
[24] M.S. Chin, B.B. Freniere, C.F. Bonney, L. Lancerotto, J.H. Saleeby, Y.C. Lo, D. P. Orgill, T.J. Fitzgerald, J.F. Lalikos, Skin perfusion and oxygenation changes in radiation fibrosis, Plast. Reconstr. Surg. 131 (4) (2013) 707–716.
[25] K. Ueda, Y. Yasuda, E. Furuya, S. Oba, Inadequate blood supply persists in keloids, Scand. J. Plast. Reconstr. Surg. Hand Surg. 38 (5) (2004) 267–271.
[26] F.W. Nangole, G.W. Agak, Keloid pathophysiology: fibroblast or inflammatory disorders? JPRAS Open 22 (2019) 44–54.
[27] H.J. Clarke, J.E. Chambers, E. Liniker, S.J. Marciniak, Endoplasmic reticulum stress in malignancy, Cancer Cell 25 (5) (2014) 563–573.
[28] G.G. Gauglitz, Management of keloids and hypertrophic scars: current and emerging options, Clin. Cosmet. Investig. Dermatol. 6 (2013) 103–114.
[29] P.D. Verhaegen, M.B. van der Wal, E. Middelkoop, P.P. van Zuijlen, Objective scar assessment tools: a clinimetric appraisal, Plast. Reconstr. Surg. 127 (4) (2011) 1561–1570.
[30] N. Kurokawa, K. Ueda, M. Tsuji, Study of microvascular structure in keloid and hypertrophic scars: density of microvessels and the efficacy of three-dimensional vascular imaging, J. Plast. Surg. Hand Surg. 44 (6) (2010) 272–277.
[31] C.W. Kischer, A.C. Thies, M. Chvapil, Perivascular myofibroblasts and microvascular occlusion in hypertrophic scars and keloids, Hum. Pathol. 13 (9) (1982) 819–824.
[32] S. Kim, H.J. Lee, K.H. Ko, A.Y. Park, J. Koh, H.K. Jung, New Doppler imaging technique for assessing angiogenesis in breast tumors: correlation with immunohistochemically analyzed microvessels density, Acta Radiol. 59 (12) (2018) 1414–1421.
[33] K.C. Lee, J. Dretzke, L. Grover, A. Logan, N. Moiemen, A systematic review of objective burn scar measurements, Burns Trauma 4 (2016) 14.
[34] D.F. Sloan, R.D. Brown, C.H. Wells, J.G. Hilton, Tissue gases in human hypertrophic burn scars, Plast. Reconstr. Surg. 61 (3) (1978) 431–436.
[35] S. Ichioka, T. Ando, M. Shibata, N. Sekiya, T. Nakatsuka, Oxygen consumption of keloids and hypertrophic scars, Ann. Plast. Surg. 60 (2) (2008) 194–197.
[36] K.X. Song, S. Liu, M.Z. Zhang, W.Z. Liang, H. Liu, X.H. Dong, Y.B. Wang, X.J. Wang, Hyperbaric oxygen therapy improves the effect of keloid surgery and radiotherapy by reducing the recurrence rate, J. Zhejiang Univ. Sci. B 19 (11) (2018) 853–862.
[37] Y. Yang, Y.G. Zhang, G.A. Lin, H.Q. Xie, H.T. Pan, B.Q. Huang, J.D. Liu, H. Liu, N. Zhang, L. Li, J.H. Chen, The effects of different hyperbaric oxygen manipulations in rats after traumatic brain injury, Neurosci. Lett. 563 (2014) 38–43.

Cheng Chen, MD, is a resident of Ultrasonography in Peking Union Medical College Hospital, China. Her fields of scientific interests: Dermatologic disease such as keloids and lymphedema, musculoskeletal disease, and multimodal Photoacoustic/Ultrasonic imaging system.

Sirui Liu is a MD candidate in the Ultrasonography Department, Peking Union Medical College Hospital, China. She focuses on the clinical application of photoacoustic imaging and multi-modality imaging, especially the clinical prompt diagnosis of diseases in obstetrics and gynecology.

Chenyang Zhao received B.S. degree in Zhongshan Medical School of Sun Yat-Sen University, and is working on M.D. degree in Department of Ultrasound, Peking Union Medical College Hospital, China. She is now working on the research of the artificial intelligence of medical imaging, the clinical translation of photoacoustic imaging, and the synthesis and application of multi-modal ultrasonic microbubbles. She has participated in a series clinical trials of breast cancer imaging and rheumatoid arthritis imaging.

Ruojiao Wang, MD, is an attending doctor of Ultrasonography in Peking Union Medical College Hospital, China. Her current research interests focus on breast disease and multimodal Photoacoustic/Ultrasonic imaging system.

Nanze Yu, MD, is an attending at the department of plastic surgery, Peking Union Medical College Hospital, China. He received his M.D. degree at Peking Union Medical College, and did his postdoctoral training at Harvard Medical School. His research interest pertains to cosmetic and reconstructive surgery.

Xiao Long, MD, is currently the Professor and Deputy Chief of Division of Plastic and Reconstructive Surgery, Peking Union Medical College Hospital, China. She has published several papers in keloid, lymphedema and adipose-derived stem cells. She is the faculty member of Chinese Society of Plastic Surgeons.

Youbin Wang, MD, is a plastic surgeon and a professor in Peking Union Medical College Hospital, China. He has focused on the field of keloid more than ten years. He has developed many surgical methods in keloid treatment and raised a new concept of “keloid subepidermal microvascular network flap" based on clinical observation and experiment study. His current study is to explore keloid development mechanism in the view of tumor immune genetics.

Yu Xia is a professor of Ultrasonography in Peking Union Medical College Hospital, China. He received his master and pH.D. degree in the field of radiology from Peking Union Medical College. During his master and pH.D. degree time, he focused himself on contrast-enhanced ultrasound imaging. After that, he dedicated himself at thyroid ultrasound research. His current research interest pertains to AI thyroid ultrasound, especially the prognosis of papillary thyroid carcinoma.

Yuxin Jiang, MD, is the head and professor of Ultrasonography in Peking Union Medical College Hospital, China. He is China Branch Chairman of International Society of Ultrasound in Obstetrics and Gynecology (ISUOG), and vice chairman of Asian Federation for Societies of Ultrasound in Medicine and Biology (AFSUMB). He has co-organized dozens of international conferences and academic activities. He is the author and translator of more than 20 books, and more than 100+ papers in the fields of ultrasonography. He is good at diagnosing difficult and complicated cases. The main field of his scientific interests is breast cancer, thyroid and parathyroid disease, and contrast-enhanced ultrasonography of liver, kidney, breast and thyroid.

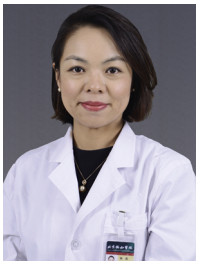

Meng Yang, MD, is a Professor of Ultrasonography in Peking Union Medical College Hospital, China. From 2011–2012, she worked as visiting professor at Molecular Imaging Program at Stanford University (MIPS). She has been the Principal Investigator of a series of national and provincial scientific projects in the field of new imaging techniques. She is the author of more than 90+ papers in the fields of ultrasonography, and she received awards from the Chinese Academy of Medicine. She has been working on the development and clinical translation of photoacoustic/ultrasound (PA/US) imaging system for 6 years. Her scientific field is the clinical transformation of multimodal photoacoustic/Ultrasonic imaging system in su perficial and obstetrics and gynecology diseases.